

INFRARED MODEL SPECTRA FOR EVOLVING RED SUPERGIANTS

Kyung-Won Suh

Department of Astronomy and Space Science
Chungbuk National University, Cheongju 360-763, Korea

(Received May 6, 1993; Accepted June 13, 1993)

ABSTRACT

The space and ground based infrared spectra of red supergiants are modeled and arranged in order of their evolutionary status with their theoretical model parameters. The chemical compositions of the dust shells around red supergiants are affected by the nuclear reactions and dredge-up processes of the central stars. Those processes are sensitively dependent on the initial mass, the initial chemical composition, and the evolutionary status. Miras, infrared carbon stars, and OH/IR stars have a close link in their evolution in many aspects, *i.e.*, the chemical composition, the optical depths and the mass loss rates. The evolutionary tracks for the three classes of red supergiants on infrared two-color diagrams have been made from model calculations and IRAS observational data.

1. INTRODUCTION

Stars lose their masses constantly after their birth, but the stellar mass loss is especially prominent in the last stages of their lives. It has been believed that red supergiants are losing their masses at rates of $10^{-8} \sim 10^{-4} M_{\odot}/\text{yr}$. They are known to be asymptotic giant branch stars that are at the end stages of the evolution for the stars with zero age main sequence masses of $1 \sim 10 M_{\odot}$. Red supergiants are often characterized by the thick dust envelopes and large amplitude pulsations. According to their energy spectra, chemical composition, they are divided into three main groups; M-type Miras, C-type carbon stars, and OH/IR stars. The purpose of this work is to clarify the evolutionary aspects in the physical parameters of the red supergiants mainly from the direct interpretation of their infrared spectra.

2. OPTICAL PROPERTIES OF DUST GRAINS AND MODEL CALCULATIONS

Optical properties of dust grains in the envelopes of Miras and OH/IR stars are investigated in detail by Suh (1991), and for carbon stars by Suh (1992). In this work, we have significantly modified the optical constants for Miras to improve the fitting with observations. Figure 1 and 2 show the absorption and scattering efficiency factors for Miras. Many authors (*e.g.*, Volk and Kwok 1988, Suh 1991) mentioned the temperature dependence of the optical constants of silicate dust grains, in this work we find more detailed shape of the changes based on the present model calculations better fitted with observations.

We have made a new set of radiative transfer model calculations for Miras to improve the fitting with observations. We have used Leung's radiative transfer code (Egan *et al.* 1988) for spherical symmetric dust shells. In the present calculations, a radial grid of 125 points and a wavelength grid of 70 points were used. The scattering is accurately considered. For Miras, the central star's temperature of 3000 K and luminosity of $10^4 L_{\odot}$ are assumed. All the procedures for the model calculations are the same as the author's previous work for Miras (Suh 1991), but in this work, the optical constants are significantly modified to improve the fitting.

Figure 3 and 4 show the new results of model calculations for Miras with different optical depths (τ) at $9.7 \mu\text{m}$ (lines) superimposed on the observational data (circles) of *o* Ceti and later M-type star IK Tau. The observational data for *o* Ceti and IK Tau are from the ground-based observation by Merrill and Stein 1976 (open circles), and IRAS observation (filled circles). The results of radiative transfer model calculations for Miras performed with present paper, for OH/IR stars by Suh (1991), and for carbon stars by Suh (1992) have been used to get theoretical model positions on infrared two-color diagrams as we will discuss in the next section.

3. THE EVOLUTION ON INFRARED TWO-COLOR DIAGRAMS

The Infrared point source photometric observations at 12, 25, 60, 100 μm made by IRAS (1986) give us the important data for many oxygen-rich and carbon-rich supergiants. To see the overall spectral changes of red supergiants, it is meaningful to consider their positions on two-color diagrams obtained from the infrared fluxes at four colors. Table 1, 2, and 3 show the theoretical values for Miras, OII/IR stars, and carbon stars obtained from radiative transfer model calculations as discussed in last section.

Figure 5 shows the infrared two-color diagram with horizontal axis for $[(\lambda F_{\lambda}(25 \mu\text{m}))]/[(\lambda F_{\lambda}(12 \mu\text{m}))]$, and perpendicular axis for $[(\lambda F_{\lambda}(60 \mu\text{m}))]/[(\lambda F_{\lambda}(25 \mu\text{m}))]$. And figure 6 shows the infrared two-color diagram with horizontal-axis for $[(\lambda F_{\lambda}(60 \mu\text{m}))]/[(\lambda F_{\lambda}(25 \mu\text{m}))]$, and perpendicular axis for $[(\lambda F_{\lambda}(100 \mu\text{m}))]/[(\lambda F_{\lambda}(60 \mu\text{m}))]$. Big symbols are from theoretical model calculations and small symbols are from IRAS observational data (IRAS 1986). Circles represent Miras, squares for OH/IR stars,

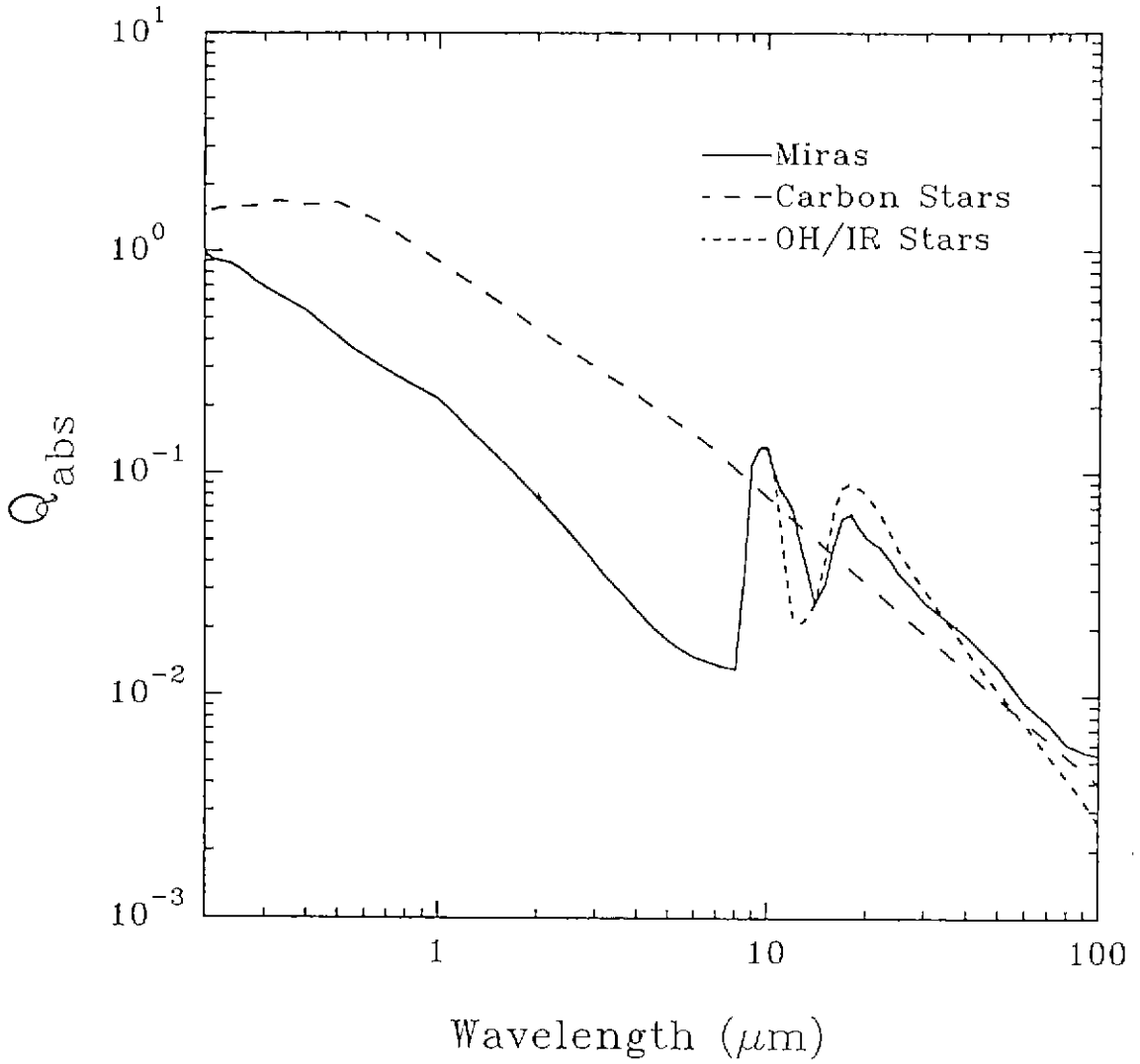


Figure 1. Absorption efficiency factors for Miras, OH/IR stars, and carbon stars.

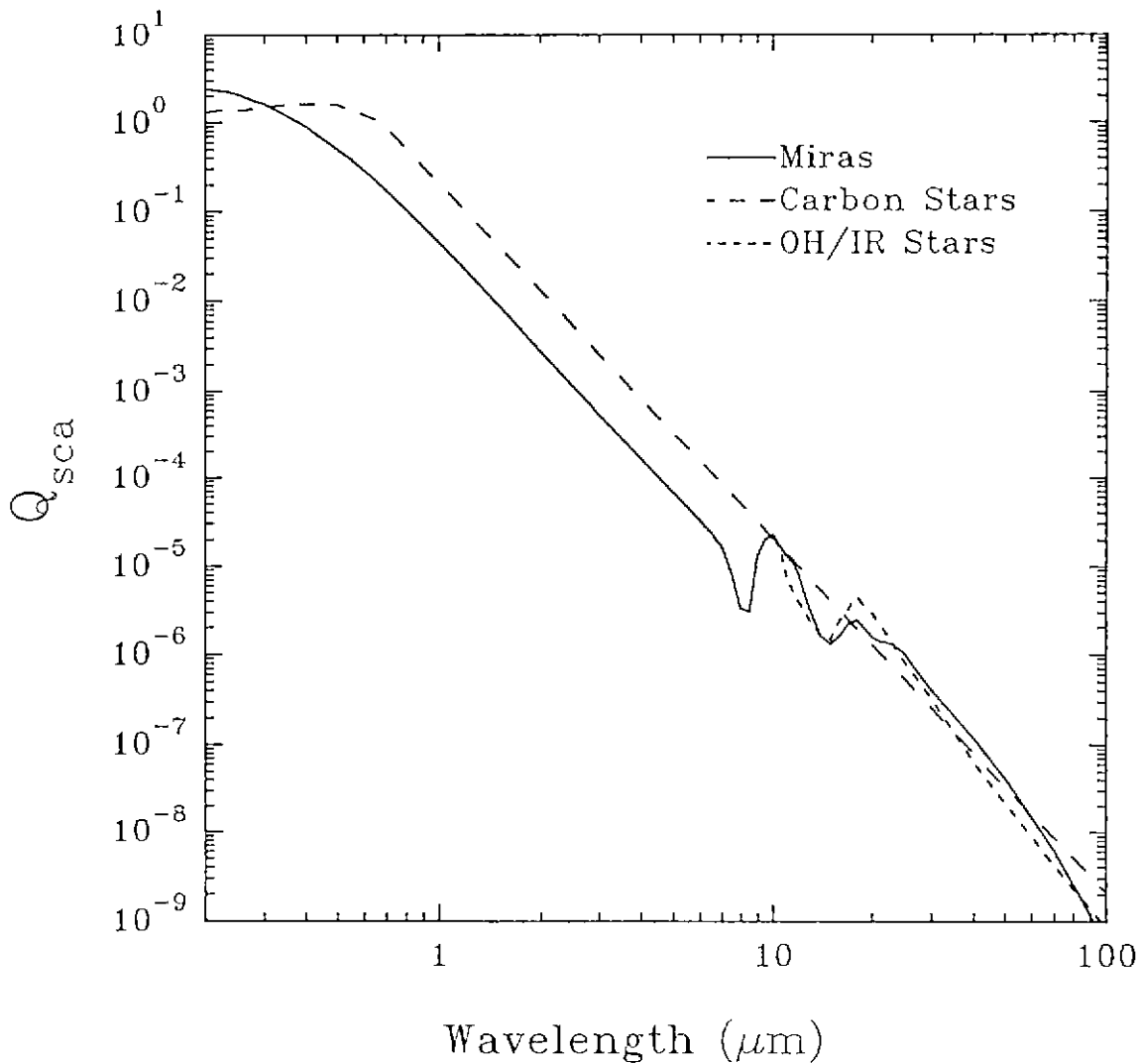


Figure 2. Scattering efficiency factors for Miras, OH/IR stars, and carbon stars.

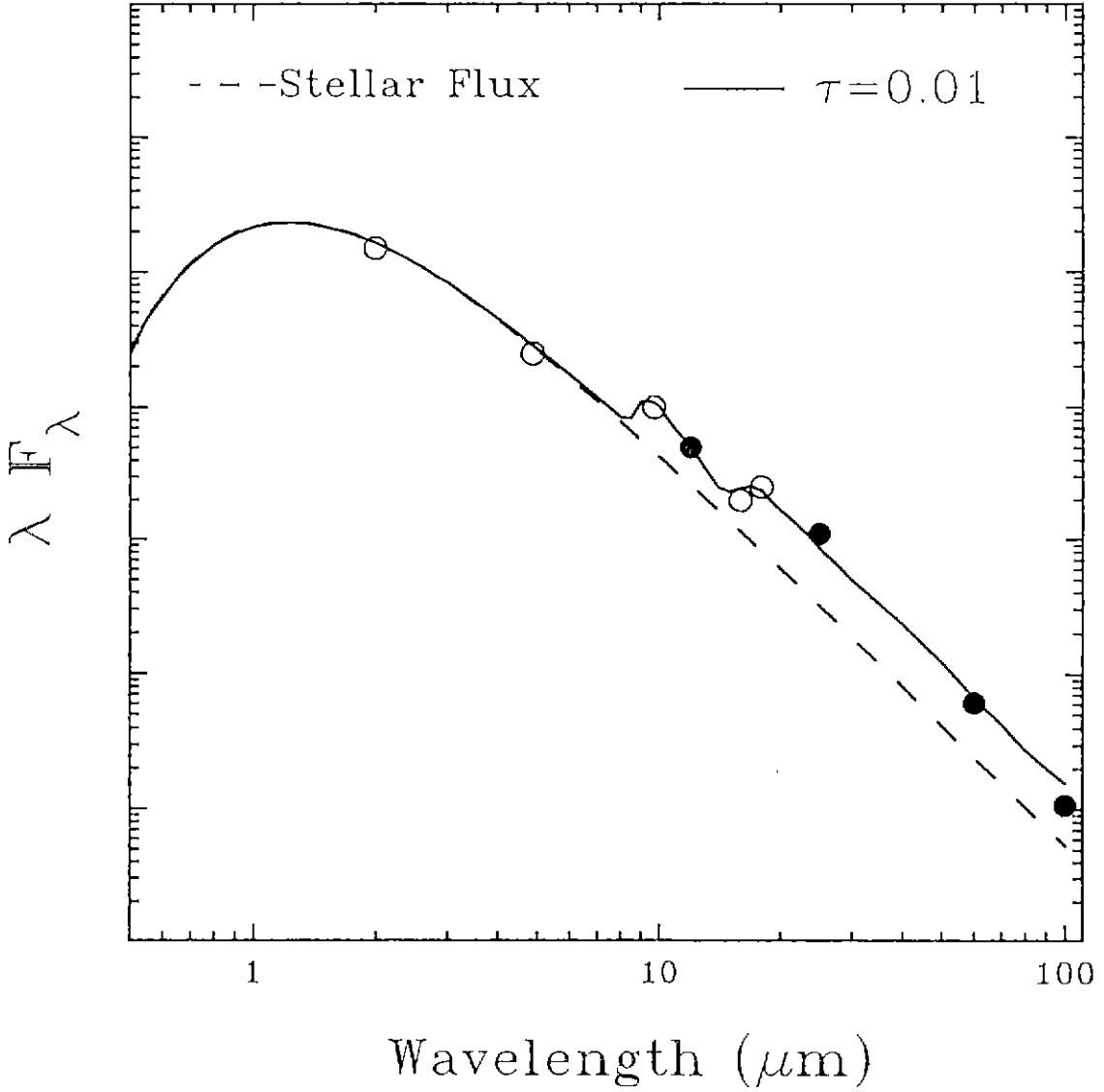


Figure 3. Results of model calculations superimposed on observations for O Ceti.

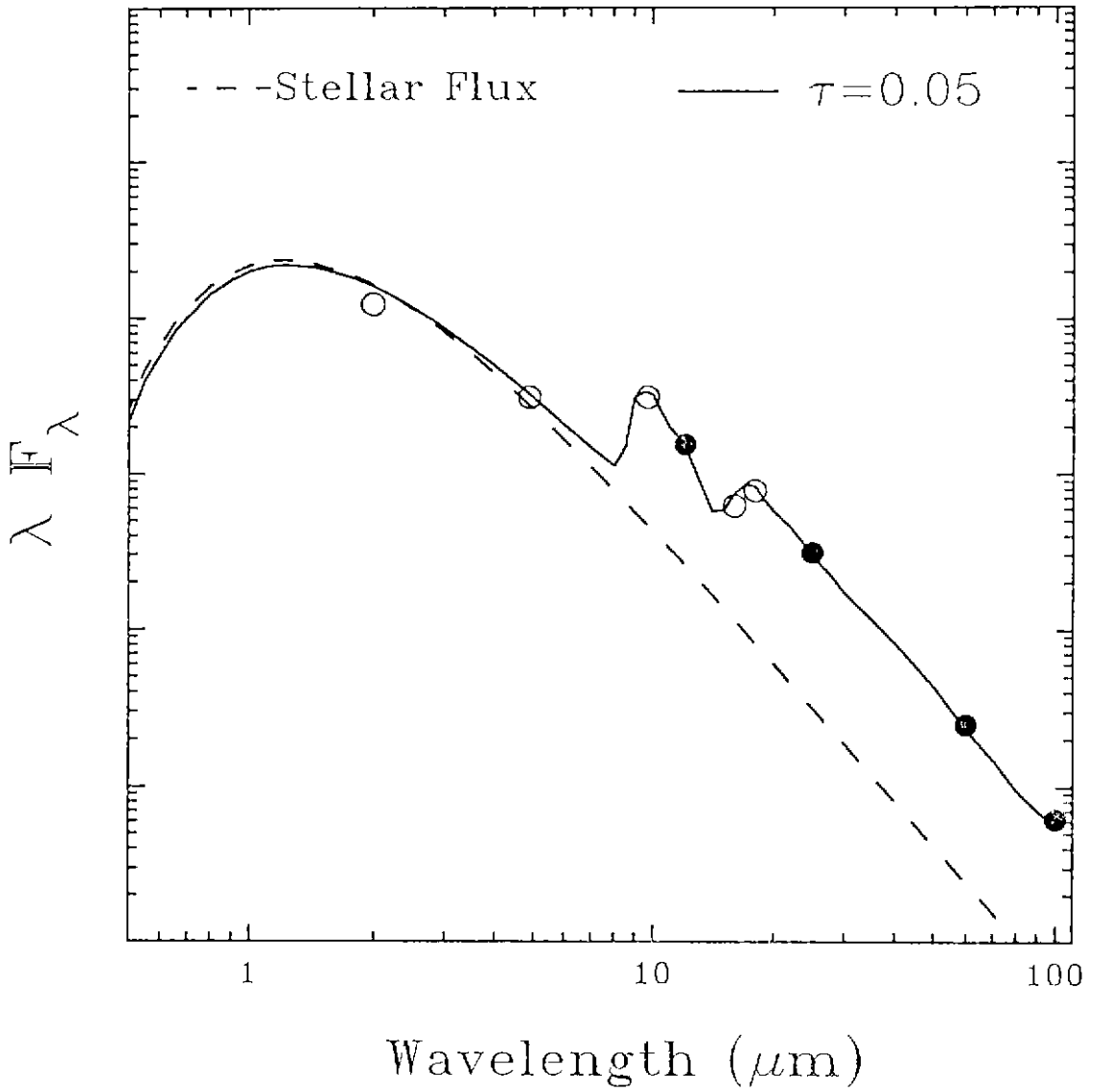


Figure 4. Results of model calculations superimposed on observations for IK Tau.

Table 1. Results of Model Calculations for Miras.

$\tau_{9.7\mu m}$	$[(\lambda F_{\lambda}(25\mu m)) / (\lambda F_{\lambda}(12\mu m))]$	$[(\lambda F_{\lambda}(60\mu m)) / (\lambda F_{\lambda}(25\mu m))]$	$[(\lambda F_{\lambda}(100\mu m)) / (\lambda F_{\lambda}(60\mu m))]$
0.001	0.13	0.077	0.22
0.01	0.17	0.078	0.23
0.05	0.2	0.079	0.24
0.5	0.24	0.085	0.26
2	0.37	0.11	0.28

Table 2. The Results of Model Calculations for OH/IR Stars.

$\tau_{9.7\mu m}$	$[(\lambda F_{\lambda}(25\mu m)) / (\lambda F_{\lambda}(12\mu m))]$	$[(\lambda F_{\lambda}(60\mu m)) / (\lambda F_{\lambda}(25\mu m))]$	$[(\lambda F_{\lambda}(100\mu m)) / (\lambda F_{\lambda}(60\mu m))]$
4	0.73	0.093	0.17
8	0.79	0.14	0.18
12	0.9	0.2	0.19
25	1	0.27	0.21
32	1.1	0.34	0.21

Table 3. The Results of Model Calculations for Carbon Stars.

$\tau_{10\mu m}$	$[(\lambda F_{\lambda}(25\mu m)) / (\lambda F_{\lambda}(12\mu m))]$	$[(\lambda F_{\lambda}(60\mu m)) / (\lambda F_{\lambda}(25\mu m))]$	$[(\lambda F_{\lambda}(100\mu m)) / (\lambda F_{\lambda}(60\mu m))]$
0.05	0.18	0.093	0.2
0.2	0.2	0.1	0.2
0.5	0.22	0.11	0.21
0.7	0.24	0.11	0.22
2	0.35	0.12	0.23
5	0.72	0.16	0.25

and triangles for carbon stars.

As the infrared re-emission processes by dust grains in circumstellar shell overwhelm the overall flux, the position on the two-color diagrams would move to right-upper direction. So we may expect that as red supergiants evolve and the optical depths of the dust shells increase, the position on the two-color diagram would move to right-upper direction if we assume that the same dust grains are just adding up and there are no conspicuous line opacities. As Miras evolve to OH/IR stars, very conspicuous emission lines at $9.7\mu\text{m}$ and $18\mu\text{m}$ change to absorption, so there is a discontinuity between the track for Miras and OH/IR stars. And as Miras evolve to carbon stars, oxygen dust grains cease forming temporarily and the new carbon dust grains begin to form, so the evolution track goes back to dust-free stars' position then move to right-upper direction continuously.

4. DISCUSSION

OH/IR stars with oxygen rich envelopes are considered to be an extension toward older age, longer periods, thicker dust envelopes and enhanced mass loss of the optically known oxygen rich M-type Mira stars. C-type carbon stars are also believed to be the evolutionary successors of M-type Mira stars that have thin oxygen-rich dust envelopes because many S-type carbon stars have oxygen rich envelopes (*e.g.* Vardya 1989).

The key factor for the different evolutionary track may be the initial mass. When the intermediate mass asymptotic giant branch stars go through the carbon dredge-up, oxygen-rich grains cease from forming and the mass loss stops temporarily and becomes visual carbon stars. After that phase, carbon grains start forming and they become infrared carbon stars with thick carbon dust envelopes and very high mass loss rates. Thermal pulse requires very high luminosity for high mass stars (Iben 1981), by the time the luminosity reaches the required one, the envelope could be completely lost. Therefore, for high mass stars, there could be no change in chemical composition of dust grains. And for low mass stars, the envelope could be very small and easily lost before the carbon dredge-up begins. Table 4 summarizes the evolutionary scenario for red supergiants.

Some carbon-rich planetary nebulae have silicate dust grains; in this case, very late carbon dredge-up happened as we may expect for the objects half way between high mass and intermediate mass scenarios. Planetary nebulae often show two, and sometimes three, shell like structures around them (*e.g.*, Balick *et al.* 1992). These may be due to abrupt changes in the mass loss rate back when the star was a dusty red giant. The red giant has long since lost its envelope and is now a nuclei of the planetary nebula, and is illuminating these past episodes of mass loss.

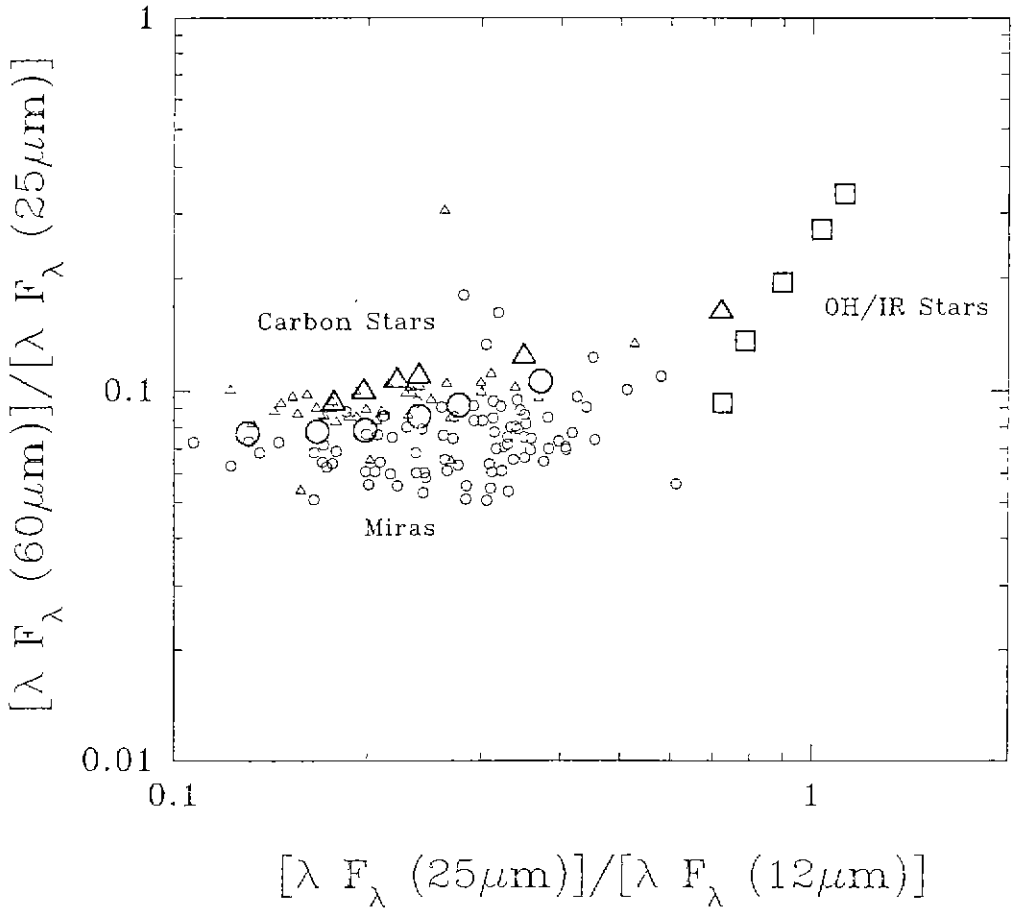


Figure 5. The infrared two-color diagram with horizontal axis for $[(\lambda F_{\lambda}(25\mu\text{m})) / (\lambda F_{\lambda}(12\mu\text{m}))]$, and perpendicular axis for $[(\lambda F_{\lambda}(60\mu\text{m})) / (\lambda F_{\lambda}(25\mu\text{m}))]$.

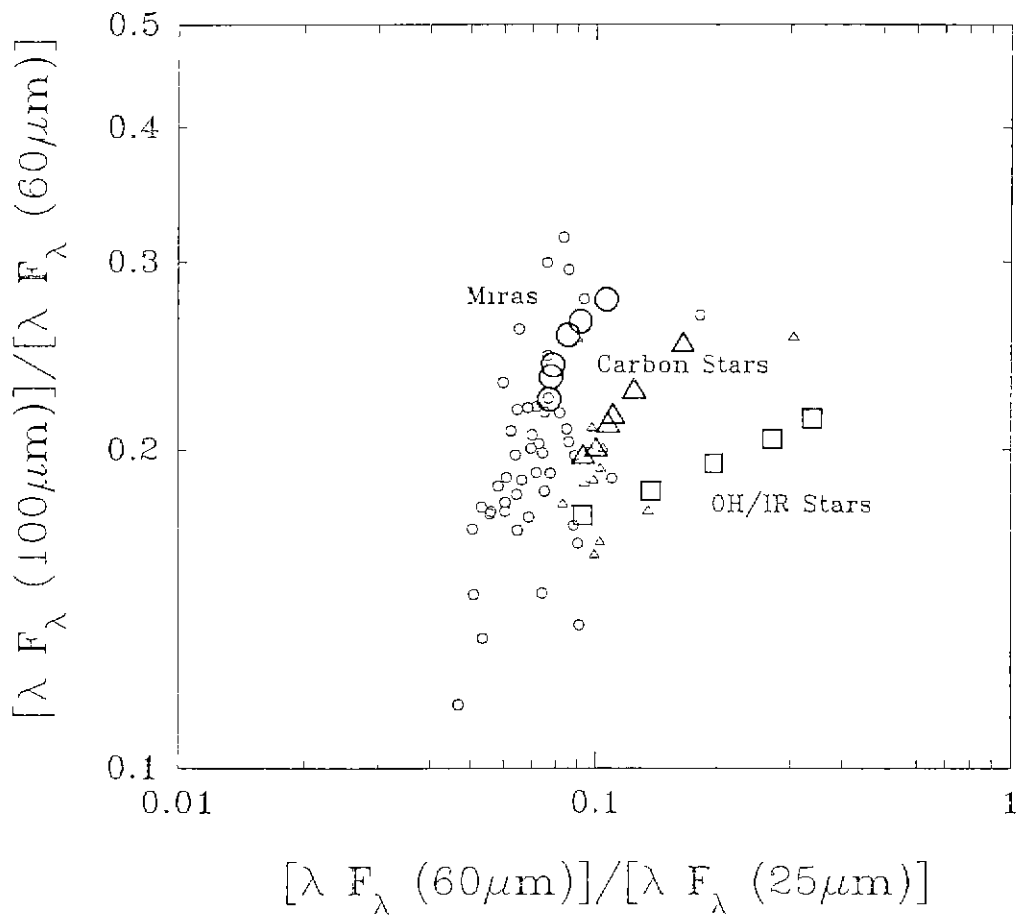


Figure 6. The infrared two-color diagram with horizontal-axis for $[(\lambda F_{\lambda}(60\mu\text{m})) / (\lambda F_{\lambda}(25\mu\text{m}))]$, and perpendicular axis for $[(\lambda F_{\lambda}(100\mu\text{m})) / (\lambda F_{\lambda}(60\mu\text{m}))]$.

Table 4. Evolutionary Scenario for Red Supergiants

Evolution to Asymptotic Giant Branch Stars ($M_{ZAMS} = 1 - 10M_{\odot}$) Oxygen rich stellar envelope Silicate dust grains form Optical Miras		
<i>Low Mass Stars</i>	<i>Intermediate Mass Stars</i>	<i>High Mass Stars</i>
Late Miras	Carbon Dredge-Up Optical Carbon Stars Carbon dust grains form Infrared Carbon Stars	OH/IR Stars
Oxygen-rich Planetary Nebulae	Carbon-rich Planetary Nebulae	Oxygen-rich Planetary Nebulae

ACKNOWLEDGEMENTS: This work was financially supported by the Chungbuk National University Research Grant. We thank for this support.

REFERENCES

- Balick, B., Gonzalez, G., Frank, A. & Jacoby, G. 1992, ApJ, 392, 582
 Egan, M. P., Leung, C. M. & Spagna, G. F. Jr. 1988, Computer Phy. Comm., 48, 271
 Iben, I. 1981, ApJ, 246, 278
 IRAS catalogues and atlases 1986, Point Source Catalogue, US Government Publication Office
 Merrill, K. M. & Stein, W. A. 1976, PASP, 88, 285
 Suh, K. W. 1991, Ap&SS, 181, 237
 Suh, K. W. 1992, JA&SS, 9, 183
 Vardya, M. S. 1989, in Evolution of Peculiar Red Giant Stars, ed. H. R. Johnson & B. Zuckerman (Cambridge: Cambridge University Press), 292
 Volk, K. & Kwok, S. 1988, ApJ, 331, 435